CONTINUOUS HYBRID NON-ZONAL RANS/LES SIMULATIONS OF TURBULENT ROTATING FLOWS USING THE PITM METHOD

Bruno Chaouat
Department of Computational Fluid Dynamics, ONERA
BP 72 - 92322 Châtillon cedex, France
Bruno.Chaouat@onera.fr

ABSTRACT

The partially integrated transport modeling (PITM) method viewed as a continuous approach of hybrid RANS/LES with seamless coupling is used to derive a subfilter-scale stress model in the framework of second moment closures (SMC) applicable in a rotating frame of reference. In this work, the pressure-strain correlation term is modeled from a physical standpoint in an invariant form under an arbitrary change of non-inertial frame of reference. As a result of the simulations, it is found that the subfilter-scale stress model reproduces fairly well the mean features of turbulent rotating channel flows performed on coarse grids with a reduction of the computational cost.

INTRODUCTION

Numerous applications in turbomachinery industry are concerned with turbulent flows in system rotation. In this framework, fully developed turbulent channel flows subjected to a spanwise rotation as shown in figure 1 have been previously studied both experimentally (Johnston et al., 1972) and numerically by several authors. Such rotating channel flows have been initially computed in the past by using Reynolds stress models (RSM) in RANS methodology (Schiestel, 2008) and then, due to the increase of computer power, by large eddy simulations (LES) for investigating the mean features of these rotating turbulent flows (Lamballais et al., 1998). These experimental and numerical studies have shown that the Coriolis forces associated with the rotation appreciably affect the mean motion and the turbulent fluctuations. In particular, as the rotation rate increases, the mean flow becomes more and more asymmetric with respect to the channel center and the turbulence activity dramatically decreases with respect to the non-rotating case. From a quantitative point of view, experimental flow visualizations as well as recent direct numerical simulations have provided the structural information on the flow.

Conventional large eddy simulations which consist of modeling the more universal small scales corresponding to the region of the spectrum located after the cutoff wave number κ_c while the resolved scales are explicitly computed by the numerical scheme are a promising method. They allow to mimic the acting mechanisms of turbulence interactions. However, most of LES simulations assume a direct constitution relation between the turbulent stress and strain components that is only valid for fine grained turbulence. On the other hand, Reynolds stress models used in RANS appear well suited for predicting engineering flows without requiring prohibitive computation times but they can not reproduce the instantaneous flow structures.

In this framework, the partially integrated transport modeling (PITM) method has been developed recently (Chaouat and Schiestel, 2005; Schiestel and Dejoan, 2005; Chaouat and Schiestel, 2007; Chaouat and Schiestel, 2009) for performing hybrid RANS/LES simulations on relatively coarse grids with seamless coupling between the RANS and LES regions, the cutoff wave number being located almost anywhere within the energy spectrum. From a theoretical point of view, the PITM method gains major interest because it bridges these two different levels of description in a consistent way by a unifying formalism developed in the spectral space (Chaouat and Schiestel, 2007). As the transport equations for the subfilter stress in terms of central moment are formally similar to the statistical equations, the PITM method can be applied to almost all statistical models to derive their hybrid LES counterparts corresponding to subfilter models, provided an adequate dissipation equation is coupled to the turbulent energy or stress transport equations. These derived subfilter models include both eddy viscosity models $k_{sfs}-\epsilon_{sfs}$ (Schiestel and Dejoan, 2005; Befeno and Schiestel, 2007) and stress models $(\tau_{ij})_{sfs}-\epsilon_{sfs}$ (Chaouat and Schiestel, 2005; Chaouat and Schiestel, 2009; Chaouat, 2010a), depending on the level of closures. The variables k_{sfs}, $(\tau_{ij})_{sfs}$ and ϵ_{sfs} denote the subfilter turbulent energy, stress and dissipation-rate, respectively. These models have been previously used for successfully simulating engineering flows on coarse grids or turbulent flows with strong departure from spectral equilibrium. In the last several years, the PITM method has become more and more widespread in turbulence modeling because of its practical interest in the field of engineering applications. But these derived models require a specific modeling to tackle engineering flows encountered in turbomachinery industry subjected to system rotation.

In this work, considering that second moment closures (SMC) constitute a convenient framework for system rotation, we propose to derive a subfilter-scale stress model $(\tau_{ij})_{sfs}-\epsilon_{sfs}$ for performing large eddy simulations of rotating turbulent flows on relatively coarse grids. This modeling strategy is motivated by the idea that the recognized advantages of second moment closures are worth transposing to subfilter-scale modeling, especially for rotating flows when the subfilter-scale (SFS) part is not small compared to the resolved part. We will show that the Coriolis term must be embedded in the subfilter stress model as a source term and that the pressure-strain-correlation term which plays a pivotal role by redistributing the turbulent energy among the different stress components can be developed in an invariant form under arbitrary time-dependent rotations of the spatial frame of reference. In this study, coarse grids are deliberately chosen to highlight the ability of the PITM method to simulate large scales of the flow with a sufficient fidelity for engineering computations.

THE FILTERING PROCESS AND GOVERNING EQUATIONS

We consider the turbulent flow of a viscous incompressible fluid. In a frame rotating at angular velocity $\boldsymbol{\Omega}$, the instantaneous momentum equation reads

$$\frac{\partial u_i}{\partial t} + \frac{\partial}{\partial x_j}(u_i u_j) = -\frac{1}{\rho}\frac{\partial p}{\partial x_i} + \nu \frac{\partial^2 u_i}{\partial x_j \partial x_j} - 2\epsilon_{ijk}\Omega_j u_k - \epsilon_{ijk}\epsilon_{kpq}\Omega_j\Omega_p x_q \tag{1}$$

where u_i, p, ϵ_{ijk}, ν are the velocity vector, the pressure, the Levi-Civita's permutation tensor, the kinematic viscosity of the fluid, respectively. The terms appearing in the right hand side of this equation are referred to as the Coriolis acceleration $-2\boldsymbol{\Omega} \times \boldsymbol{u}$, and centrifugal acceleration $-\boldsymbol{\Omega} \times (\boldsymbol{\Omega} \times \boldsymbol{x})$. In large eddy simulations, the flow variable ϕ is decomposed into a resolved scale part $\bar{\phi}$ including the statistical mean $\langle\phi\rangle$ and the large scale $\phi^< = \bar{\phi} - \langle\phi\rangle$ and a subfilter-scale (or modeled) fluctuating part ϕ'. The resolved variable $\bar{\phi}$ is defined by the filter function G_Δ as

$$\bar{\phi}(\boldsymbol{x}) = \iiint_{\mathcal{D}} G_\Delta(\boldsymbol{x} - \boldsymbol{x}')\,\phi(\boldsymbol{x}')\,d^3x' \tag{2}$$

where Δ is the filter width. Applying the filtering operation to the instantaneous momentum equation yields the filtered equation

$$\frac{\partial \bar{u}_i}{\partial t} + \frac{\partial}{\partial x_j}(\bar{u}_i \bar{u}_j) = -\frac{1}{\rho}\frac{\partial \bar{p}}{\partial x_i} + \nu \frac{\partial^2 \bar{u}_i}{\partial x_j \partial x_j} - \frac{\partial (\tau_{ij})_{sfs}}{\partial x_j} - 2\epsilon_{ijk}\Omega_j \bar{u}_k - \epsilon_{ijk}\epsilon_{kpq}\Omega_j\Omega_p x_q \tag{3}$$

where $(\tau_{ij})_{sfs}$ denotes the subfilter scale stress tensor defined by the mathematical relation

$$(\tau_{ij})_{sfs} = \overline{u_i u_j} - \bar{u}_i \bar{u}_j \tag{4}$$

The presence of the turbulent contribution $(\tau_{ij})_{sfs}$ in equation (3) indicates the effect of the subfilter-scales to the resolved field. The resolved scale tensor is computed by the relation

$$(\tau_{ij})_{les} = \bar{u}_i \bar{u}_j - \langle u_i\rangle\langle u_j\rangle \tag{5}$$

Assuming that the large and small scale fluctuations are uncorrelated as for spectral cutoff filter defined by the Fourier transform, the Reynolds stress τ_{ij} then reads

$$\tau_{ij} = \langle(\tau_{ij})_{sfs}\rangle + \langle(\tau_{ij})_{les}\rangle \tag{6}$$

The closure of the filtered momentum equation (3) requires to model the subfilter-scale turbulent stress $(\tau_{ij})_{sfs}$. In the framework of second moment closures, this is made by means of its transport equation which is the required level for accurately reproducing the physical processes of turbulent flows.

PARTIAL INTEGRATED TRANSPORT MODELING METHOD

Principle of the method

The PITM method finds its basic foundation in the spectral space by considering the Fourier transform of the two-point fluctuating velocity correlation equations in homogeneous turbulence. The extension to non-homogeneous turbulence is developed within the approximate framework of the tangent homogeneous space at a point of a non-homogeneous flow field assuming Taylor series expansion in space for the mean velocity field (Chaouat and Schiestel, 2007). When transposing the spectral equation in the physical space by inverse Fourier transform involving a partial integration of the turbulent field in the range $[\kappa_c, \kappa_d[$ where $\kappa_c = \pi/\Delta$ is the cutoff wave number computed by the grid size width Δ, and κ_d is the dissipative wave number placed at the end of the inertial range of the spectrum completely after the transfer zone, one can derive a subfilter-scale model based on the transport equations for the subfilter-scale stresses $(\tau_{ij})_{sfs}$ and the dissipation rate ϵ_{sfs} that looks formally like the corresponding RANS/RSM model but the coefficients used in the model are no longer constants. They are now some functions of the dimensionless parameter η_c involving the cutoff wave number κ_c and the turbulent length scale L_e built using the total turbulent kinetic energy k, the subfilter dissipation rate ϵ_{sfs} and the large scale dissipation rate denoted $\epsilon^<$

$$\eta_c = \kappa_c L_e = \frac{\pi\, k^{3/2}}{\Delta^{1/3}\,(\langle\epsilon_{sfs}\rangle + \langle\epsilon^<\rangle)} \tag{7}$$

In PITM methodology, the subfilter-scale stress model varies continuously with respect to the ratio of the turbulent length-scale to the grid-size L_e/Δ. Note that a formalism based on temporal filtering has been proposed recently to handle non-homogeneous flows leading to a variant of the PITM method called TPITM method (Fadai-Ghotbi et al., 2010a).

Exact transport equations in presence of rotation

The first step of the present approach consists of writing the exact transport equation of the subfilter-scale stress $(\tau_{ij})_{sfs}$ in presence of rotation. By using the material derivative operator $D/Dt = \partial/\partial t + \bar{u}_k \partial/\partial x_k$, the transport equation of the subfilter stress tensor can be therefore written in the simple compact form as

$$\frac{D(\tau_{ij})_{sfs}}{Dt} = P_{ij} + \Pi_{ij} + J_{ij} - (\epsilon_{ij})_{sfs} \tag{8}$$

where the terms appearing in the right-hand side of this equation are identified as production, redistribution, diffusion and dissipation. The production term P_{ij} is composed by the term P^1_{ij} produced by the interaction between the subfilter stress and the filtered velocity gradient

$$P^1_{ij} = -(\tau_{ik})_{sfs}\frac{\partial \bar{u}_j}{\partial x_k} - (\tau_{jk})_{sfs}\frac{\partial \bar{u}_i}{\partial x_k}\,, \tag{9}$$

and by the term P^2_{ij} generated by the rotation involving the Coriolis forces

$$P^2_{ij} = -2\Omega_p\left(\epsilon_{jpk}(\tau_{ki})_{sfs} + \epsilon_{ipk}(\tau_{kj})_{sfs}\right) \tag{10}$$

The exact expressions of the redistribution Π_{ij}, diffusion J_{ij} and dissipation rate $(\epsilon_{ij})_{sfs}$ appearing on the right-hand side of equation (8) are the following

$$\Pi_{ij} = \frac{2}{\rho}\,\Phi\,(p, S_{ij})\,, \tag{11}$$

$$J_{ij} = -\frac{\partial\Phi(u_i,u_j,u_k)}{\partial x_k} - \frac{1}{\rho}\frac{\partial\Phi(p,u_i)}{\partial x_j} - \frac{1}{\rho}\frac{\partial\Phi(p,u_j)}{\partial x_i} + \nu\frac{\partial^2\Phi(u_i,u_j)}{\partial x_k \partial x_k} \tag{12}$$

$$(\epsilon_{ij})_{sfs} = 2\nu\,\Phi\left(\frac{\partial u_i}{\partial x_k}, \frac{\partial u_j}{\partial x_k}\right) \tag{13}$$

where in equations (11), (12), (13), the functions Φ of two or three variables are defined by $\Phi(f,g) = \overline{fg} - \bar{f}\bar{g}$ and $\Phi(f,g,h) = \overline{fgh} - \bar{f}\Phi(g,h) - \bar{g}\Phi(h,f) - \bar{h}\Phi(f,g) - \bar{f}\bar{g}\bar{h}$ applicable for any turbulent quantities f, g, h. The quantity S_{ij} appearing in equation (11) denotes the strain deformation

$$S_{ij} = \frac{1}{2}\left(\frac{\partial u_i}{\partial x_j} + \frac{\partial u_j}{\partial x_i}\right) \tag{14}$$

Modeling of the subfilter-scale stress transport equation in presence of rotation

Contrary to the production term P_{ij} which is exact, the redistribution, diffusion and dissipation terms need to be modeled in the wave number range $[\kappa_c, \kappa_d]$. The present formalism (Chaouat and Schiestel, 2007) shows clearly the formal analogy between the statistical and filtered approaches and their compatibility. As a consequence, the closure approximations used for the statistical partially averaged equations are assumed to prevail also in the case of large eddy numerical simulations. As it was emphasized in second-moment closures, the pressure-strain correlation term Π_{ij} plays a pivotal role by redistributing the turbulent energy among the stress components allowing a more realistic description of the flow anisotropy than eddy viscosity models, and also a better account of history and nonlocal effects. It requires a specific modeling to account for the rotation. This term defined in equation (11) can be reduced to the pressure-strain subfilter fluctuating correlations in a first approximation

$$\Pi_{ij} = 2\Phi(p, S_{ij})/\rho \approx 2\overline{p' S'_{ij}}/\rho \tag{15}$$

In system rotation, it is simple matter to show that the subfilter-scale fluctuating pressure p' is solution of the Poisson equation that reads

$$\frac{1}{\rho}\frac{\partial^2 p'}{\partial^2 x_i} = -\frac{\partial^2}{\partial^2 x_j}\left[u'_i u'_j - (\tau_{ij})_{sfs}\right] - 2\left(\frac{\partial \bar{u}_i}{\partial x_j} + \epsilon_{ikj}\Omega_k\right)\frac{\partial u'_j}{\partial x_i} \tag{16}$$

Like in RANS statistical modeling, when integrating this equation in space in absence of boundaries, using the Green's function solution and then multiplying by the fluctuating strain S'_{ij}, it is found that Π_{ij} can be decomposed into a slow part Π^1_{ij} and a rapid part Π^2_{ij} as follows

$$\Pi^1_{ij}(\boldsymbol{x}) = \frac{1}{2\pi}\int_{\mathcal{D}} \overline{\frac{\partial^2}{\partial x_m \partial x_k}\left[u'_k u'_m - (\tau_{km})_{sfs}\right](\boldsymbol{x}')S'_{ij}(\boldsymbol{x})}\frac{d^3x'}{r} \tag{17}$$

$$\Pi^2_{ij}(\boldsymbol{x}) = \frac{1}{\pi}\int_{\mathcal{D}} \overline{\left[\left(\frac{\partial \bar{u}_k}{\partial x_m} + \epsilon_{kpm}\Omega_p\right)\frac{\partial u'_m}{\partial x_k}\right](\boldsymbol{x}')S'_{ij}(\boldsymbol{x})}\frac{d^3x'}{r} \tag{18}$$

where $r = |\boldsymbol{x} - \boldsymbol{x}'|$. These equations clearly show that the slow term Π^1_{ij} characterizes the return to isotropy due to the action of turbulence on itself whereas the rapid term Π^2_{ij} describes the return to isotropy by action of the absolute filtered velocity gradient involving the rotation defined by

$$\frac{\partial_a \bar{u}_k}{\partial x_l} = \frac{\partial \bar{u}_k}{\partial x_l} + \epsilon_{kpl}\Omega_p \tag{19}$$

In the present case, these terms Π^1_{ij} and Π^2_{ij} are modeled assuming that the usual statistical Reynolds stress model (Chaouat, 2005) must be recovered in the limit of vanishing cutoff wave number κ_c ($\kappa_c \to 0$). Considering that the small scales return more rapidly to isotropy than the large scales before cascading into smaller scales by non-linear interactions, Π^1_{ij} reads

$$\Pi^1_{ij} = -c_{sfs_1}\frac{\epsilon_{sfs}}{k_{sfs}}\left((\tau_{ij})_{sfs} - \frac{2}{3}k_{sfs}\,\delta_{ij}\right) \tag{20}$$

where c_{sfs_1} is an increasing function of the parameter η_c. The second term Π^2_{ij} is modeled taking into account the absolute filtered velocity gradient leading to the result (Launder et al., 1987)

$$\Pi^2_{ij} = -c_2\left(P^1_{ij} + \frac{1}{2}P^2_{ij} - \frac{1}{3}P^1_{mm}\,\delta_{ij}\right) \tag{21}$$

where the coefficient c_2 remains the same as in statistical modeling. The diffusion term J_{ij} appearing in equation (8) due to the fluctuating velocities and pressure together with the molecular diffusion, is modeled assuming a gradient law hypothesis

$$J_{ij} = \frac{\partial}{\partial x_k}\left(\nu\frac{\partial(\tau_{ij})_{sfs}}{\partial x_k} + c_s\frac{k_{sfs}}{\epsilon_{sfs}}(\tau_{kl})_{sfs}\frac{\partial(\tau_{ij})_{sfs}}{\partial x_l}\right) \tag{22}$$

where c_s is a numerical coefficient set to 0.22. Closures of equation (8) require to model the subfilter tensorial dissipation rate $(\epsilon_{ij})_{sfs}$ which is approached by $2/3\epsilon\delta_{ij}$. The modeling of the dissipation-rate ϵ_{sfs} is made in the present case by means of its transport equation. This allows to obtain an accurate estimate of the subfilter dissipation rate even in situation of non-equilibrium flows when the grid-size is no longer a good estimate of the characteristic turbulence length-scale. As a result of the theory developed in the spectral space (Chaouat and Schiestel, 2007), the fluctuating modeled transport equation for the subfilter-scale dissipation-rate ϵ_{sfs} reads

$$\frac{D\epsilon_{sfs}}{Dt} = c_{sfs\epsilon_1}\frac{\epsilon_{sfs}}{k_{sfs}}P - c_{sfs\epsilon_2}\frac{\epsilon^2_{sfs}}{k_{sfs}} + J_\epsilon \tag{23}$$

where $P = P^1_{mm}/2$. The coefficient $c_{sfs\epsilon_1}$ is constant whereas the coefficient $c_{sfs\epsilon_2}$ appearing in equation (23) is now a function of the ratio to the subfilter energy to the total energy $\langle k_{sfs}\rangle/k$ as follows (Chaouat and Schiestel, 2007)

$$c_{sfs\epsilon_2} = c_{\epsilon_1} + \frac{\langle k_{sfs}\rangle}{k}\left(c_{\epsilon_2} - c_{\epsilon_1}\right) \tag{24}$$

and where the coefficients c_{ϵ_1} and c_{ϵ_2} appearing in this equation denote the usual constants used in the statistical dissipation rate transport equation. The theory shows that the coefficients of the production term remain the same for both RANS and LES dissipation-rate equations $c_{sfs\epsilon_1} = c_{\epsilon_1} = 3/2$. In the present case, the values retained are $c_{\epsilon_1} = 1.50$ and $c_{\epsilon_2} = 1.90$. Equation (23) using the relation (24) constitutes the main feature of the PITM approach where only the part of the spectrum for $\kappa > \kappa_c$ is modeled. The ratio k_{sfs}/k appearing in equation (24) is evaluated by means of an accurate energy spectrum $E(\kappa)$ leading to the result (Chaouat and Schiestel, 2009)

$$c_{sfs\epsilon_2}(\eta_c) = c_{\epsilon_1} + \frac{c_{\epsilon_2} - c_{\epsilon_1}}{\left[1 + \beta_\eta\,\eta_c^3\right]^{2/9}} \tag{25}$$

Equation (25) indicates that the function $c_{sfs\epsilon_2}$ acts like a dynamical parameter which controls the spectral distribution of turbulence and verifies the limiting behaviors $lim_{\ \eta_c\to 0}\ c_{sfs\epsilon_2}(\eta_c) = c_{\epsilon_2}$, implying that the model behaves like a RANS/RSM whereas $lim_{\ \eta_c\to\infty} c_{sfs\epsilon_2}(\eta_c) = c_{\epsilon_1}$ means that the computation switches to DNS (or under resolved DNS if the grid-size is not enough refined). The theoretical value of the coefficient β_η in equation (25) is $\beta_{\eta\mathcal{T}} = (2/3C_K)^{9/2}$ where C_K is the Kolmogorov constant. In practice, this value is optimized for $C_K = 1.3$ according to previous flow simulations. The diffusion term J_ϵ appearing on the left hand side of equation (23) is modeled assuming a well-known gradient law hypothesis

$$J_\epsilon = \frac{\partial}{\partial x_j}\left(\nu\frac{\partial \epsilon_{sfs}}{\partial x_j} + c_\epsilon\frac{k_{sfs}}{\epsilon_{sfs}}(\tau_{jm})_{sfs}\frac{\partial \epsilon_{sfs}}{\partial x_m}\right) \tag{26}$$

where the coefficient c_ϵ is set to 0.18.

Invariance of the subfilter-scale pressure-strain correlation term

In this section, we examine the transformation of the exact and modeled pressure-strain terms Π_{ij} under an arbitrary time-dependent rotation and a translation of the spatial frame of reference and shift of the origin of time t given by

$$\boldsymbol{x}^* = \boldsymbol{Q}(t)\,\boldsymbol{x} + \boldsymbol{b}(t), \quad t* = t + c \tag{27}$$

where c is a constant coefficient, $\boldsymbol{b}$ is a time-dependent vector and $\boldsymbol{Q}$ is any time-dependent proper orthogonal tensor verifying the well known relation

$$\dot{Q}_{km} Q_{lm} = -\dot{Q}_{lm} Q_{km} = \epsilon_{mkl}\Omega_m \tag{28}$$

The approach developed in RANS methodology (Speziale, 1979; Speziale, 1980) is transposed to the PITM method. We compute first the mean velocity as well as the fluctuating velocity under the change of frame of reference given by equation (27). As a result, the instantaneous velocity transforms as

$$u_i^* = Q_{im} u_m + \dot{Q}_{im} x_m + \dot{b}_i \tag{29}$$

whereas the filtered velocity $\bar{u}_i$ is then obtained by applying the general definition (2) leading to the result

$$\overline{u_i^*} = Q_{im} \bar{u}_m + \dot{Q}_{im} \bar{x}_m + \dot{b}_i \tag{30}$$

for the particular case of isotropic filters. The subgrid fluctuating velocity is then obtained by subtracting equation (30) from equation (29)

$$u_i'^* = Q_{im} u_m' \tag{31}$$

showing that it is frame-indifferent. The mean and fluctuating pressures remain frame-indifferent as a consequence of the principle of material frame-indifference. By using the chain rule of differentiation,

$$\frac{\partial}{\partial x_i^*} = \frac{\partial x_m}{\partial x_i^*} \frac{\partial}{\partial x_m} = Q_{im} \frac{\partial}{\partial x_m} \ , \tag{32}$$

the mean strain transforms as

$$\overline{S_{ij}^*} = Q_{im} Q_{jn} \overline{S}_{mn} \tag{33}$$

As a result (Chaouat, 2011), the exact pressure-strain term Π_{ij}^* remains invariant under a change of frame since it obeys the tensor transformation rule as follows

$$\Pi_{ij}^* = \Phi(p^*, S_{ij}^*) = Q_{im} Q_{jn} \Pi_{mn} \tag{34}$$

Now, we examine the transformation of the modeled pressure-strain term Π_{ij}. It can be expressed as a function of the anisotropy tensor $a_{ij} = ((\tau_{ij})_{sfs} - 2/3 k_{sfs}\delta_{ij})/k_{sfs}$, the mean strain term S_{ij} and the absolute vorticity tensor W_{ij} defined by

$$\overline{W}_{ij} = \frac{1}{2}\left(\frac{\partial_a \bar{u}_i}{\partial x_j} - \frac{\partial_a \bar{u}_j}{\partial x_i}\right) = \omega_{ij} + \epsilon_{mji}\Omega_m \tag{35}$$

where ω_{ij} denotes the relative vorticity. This term $\Pi_{ij}^* = \Pi(a_{ij}^*, S_{ij}^*, W_{ij}^*)$ is determined by computing a_{ij}^*, S_{ij}^* and W_{ij}^*, respectively. Applying the tensor rule (30), one can show (Chaouat, 2011) that $(\tau_{ij})_{sfs}$ transforms as

$$\begin{aligned}(\tau_{ij}^*)_{sfs} &= Q_{im} Q_{jp} (\tau_{mp})_{sfs} + Q_{im}\dot{Q}_{jp}\left[\overline{u_m x_p} - \bar{u}_m x_p\right] \\ &+ Q_{jm}\dot{Q}_{ip}\left[\overline{x_m u_p} - x_m \bar{u}_p\right] + \dot{Q}_{im}\dot{Q}_{jp}\left[\overline{x_m x_p} - x_m x_p\right]\end{aligned} \tag{36}$$

Equation (36) indicates that the subfilter stress $(\tau_{ij}^*)_{sfs}$ depends on the motion of the frame of reference through the rotation but is frame indifferent through the translation. This result is different from what would be guessed from physical intuition. But one can argue that the additional terms appearing in the right hand side of equation (36) are small in comparison with the first term so that in a first approximation, $(\tau_{ij}^*)_{sfs}$ can be reduced to

$$(\tau_{ij}^*)_{sfs} \approx Q_{im} Q_{jp} (\tau_{mp})_{sfs} \tag{37}$$

By using equation (32), it can be shown that the absolute filtered vorticity tensor $\overline{W}_{ij}^*$ transforms as

$$\overline{W_{ij}^*} = Q_{im} Q_{jp} \overline{W}_{mp} \tag{38}$$

thanks to equation (28). Taking into account equations (33), (37) and (38), we finally find that the modeled pressure-strain correlation term Π_{ij} transforms as

$$\boldsymbol{\Pi}^* = \boldsymbol{\Pi}(\boldsymbol{Q}\boldsymbol{a}\boldsymbol{Q}^T, \boldsymbol{Q}\overline{\boldsymbol{S}}\boldsymbol{Q}^T, \boldsymbol{Q}\overline{\boldsymbol{W}}\boldsymbol{Q}^T) \approx \boldsymbol{Q}\boldsymbol{\Pi}(\boldsymbol{a}, \overline{\boldsymbol{S}}, \overline{\boldsymbol{W}})\boldsymbol{Q}^T \tag{39}$$

In a mathematical sens, equation (39) means that Π_{ij} is an isotropic tensor function of its arguments (Speziale et al., 1991). Consequently, the modeled pressure-strain correlation term transforms like the exact pressure-strain correlation term, provided however that the approximation (37) is conceded in PITM methodology.

NUMERICAL METHOD AND CONDITIONS OF COMPUTATIONS

Numerical method

The numerical simulations are performed using a research code (Chaouat, 2010b) which is based on a finite volume technique. The governing equations are integrated in time by a Runge-Kutta scheme of fourth-order accuracy and the convective fluxes at the interfaces are computed by a quasi-centered numerical scheme of second-order accuracy in space. In practice, with the aim to avoid the model to reach a purely RANS or LES limiting behavior during the transition phase, a dynamical procedure (Fadai-Ghotbi et al., 2010b) has been activated during the computations. The computational domain is of dimension $3\delta \times 2\delta \times \delta$ in the streamwise, spanwise and normal directions, respectively x_1, x_2, x_3 and the rotation vector is oriented along the spanwise direction as seen in figure 1. The present simulations are performed on a coarse mesh $24\times48\times64$ and on a medium mesh $84\times64\times64$ at the Reynolds number $R_\tau = u_\tau\delta/2\nu = 386$, based on the friction velocity u_τ and the channel half width $\delta/2$ or, equivalently, at the Reynolds number $R_m = u_m\delta/\nu \approx 14000$ based on the bulk velocity u_m. The grid spacing Δ_i^+ in the periodic directions are $\Delta_1^+ \approx 96.5$, $\Delta_2^+ \approx 32.2$ and $\Delta_1^+ \approx 27.5$, $\Delta_2^+ \approx 24.1$, respectively for the coarse and medium meshes.

RESULTS AND DISCUSSION

Different values of the rotation number $Ro_m = \Omega\delta/u_m$ varying from moderate and high rotation regimes $Ro_m = 0.17$ and 0.50 are considered in this work. Note that in the literature, rotating flows are sometimes characterized by the Rossby number defined by $Rg_m = 3u_m/\delta\Omega$ which is directly related to the rotation number $Rg_m = 3/Ro_m$. The PITM results including the velocities and stresses are compared with the data of highly resolved LES simulations (Lamballais et al., 1998) using the spectral-dynamic model derived from the eddy-damped quasi normal Markovian statistical theory (EDQNM). Figures 2 and 3 show the mean dimensionless velocity profiles normalized by the bulk velocity $\langle u_1 \rangle / u_m$ versus the global coordinates for both rotation regimes and for the coarse and medium meshes. As expected, the mean velocity presents an asymmetric character which is more pronounced as the rotation regime increases from $Ro_m = 0.17$ to 0.50. Even for the coarse grid resolution, one can see that both PITM simulations provide velocity profiles in good agreement with the reference data. In particular, one can notice that the mean velocity profile exhibits a linear region of constant shear stress. The computations indicate that the slope of the mean velocity gradient $\partial \langle u_1 \rangle / \partial x_3$ is approximately equal to $2\Omega_2$, and corresponds to a nearly-zero mean spanwise absolute vorticity vector, i.e., $\langle W_2 \rangle = \langle \omega_2 \rangle + 2\Omega_2 \approx 0$. Figure 4 displays the subfilter, resolved and Reynolds turbulent shear stresses for the PITM simulations performed at $Ro_m = 0.50$. It can be shown that the subfilter stress model behaves more or less like the RANS/RSM model in the near wall region, although the grid is very refined in the normal direction to the wall, and like LES in the core flow. Obviously, the sharing out of the turbulent energy between the modeled and resolved energies is modified according to the grid spacing but not the total energy which agrees well with the reference data. More precisely, the SFS part of the shear stress is larger for the coarse mesh than the one observed for the medium mesh whereas the reverse situation occurs for the resolved part of the shear stress. Figure 5 shows the streamwise, spanwise and normal turbulent stresses for the PITM2 simulation performed at $Ro_m = 0.50$ on the medium grid. Overall, a relatively good agreement is observed with the reference data. It can be noted that the flow anisotropy is well reproduced thanks to the pressure-strain correlation term that redistributes the energy among the different stress components. This term appearing only in second-moment closures demonstrates the usefulness of the present sufbilter stress model providing a more realistic flow prediction than viscosity-based subfilter-scale models. Figure 6 shows the isosurfaces of instantaneous vorticity modulus, illustrating the dynamical elements of the flow in wall turbulence. Although the grid is very coarse, the computation succeeds in reproducing qualitatively these structures even if the grid resolution is not really sufficient in the streamwise and spanwise directions to get quantitative results obtained by DNS or highly resolved LES

CONCLUSION

The partially integrated transport modeling (PITM) method has been reconsidered for devising a subfilter-scale stress model to account for rotation in the framework of second moment closures (SMC). As a result, it has been found that the present PITM simulations performed on both coarse and medium meshes have reproduced fairly well the mean features of turbulent rotating channel flows at moderate and high rotation regimes, allowing a drastic saving of computational cost in comparison with highly resolved LES.

REFERENCES

Befeno, I. and Schiestel, R., 2007, "Non-Equilibrium Mixing of Turbulence Scales using a Continuous Hybrid RANS/LES Approach", *Turbulence and Combustion*, Vol. 78, pp. 129-151.

Chaouat, B., and Schiestel, R., 2005, "A New Partially Integrated Transport Model for Subgrid-Scale Stresses and Dissipation Rate for Turbulent Developing Flows", *Physics of Fluids*, Vol. 17, (065106).

Chaouat, B., and Schiestel, R., 2007, "From Single-Scale Turbulence Models to Multiple-Scale and Subgrid-Scale Models by Fourier Transform", *Theoretical and Computational Fluid Dynamics*, Vol. 21, n°3, pp. 201-229.

Chaouat, B., and Schiestel, R., 2009, "Progress in Subgrid-Scale Transport for Continuous Hybrid Non-Zonal RANS/LES Simulations", *International Journal of Heat and Fluid Flow*, Vol. 30, pp. 602-616.

Chaouat, B., 2010a, "Subfilter Scale Transport Model for Hybrid RANS/LES Simulations Applied to a Complex Flow", *Journal of Turbulence*, Vol. 11, n°51, pp. 1-30.

Chaouat, B., 2010b, "An Efficient Numerical Method for RANS/LES Turbulent Simulations using Subfilter Scale Transport Equation", *International Journal for Numerical Methods in Fluids*, DOI: 10.1002/fld.2421, pp.1-27.

Chaouat, B., 2011, "A New Subfilter Scale Stress Model Derived from the Partially Integrated Transport Modeling Method for Simulations of Rotating Turbulent Flows", *Submitted to Physics of Fluids*

Fadai-Ghotbi, A., Friess, C., Manceau, T. B. Gatski and Borée, J., 2010a, "Temporal Filtering: A Consistent Formalism for Seamless Hybrid RANS/LES Modeling in Inhomogeneous Turbulence", *International Journal of Heat and Fluid Flow*, Vol. 31, pp. 378-389.

Fadai-Ghotbi, A., Friess, C., Manceau, R. and Borée, J., 2010b, "A Seamless Hybrid RANS/LES Model Based on Transport Equations for the Subgrid Stresses and Ellipting Blending ", *Physics of Fluids*, Vol. 22, (055104).

Johnston, J. P., Halleen, R. M. and Lezius, D. K., 1972, "Effect of Spanwise Rotation on the Structure of Two-Dimensional Fully Developed Turbulent Channel Flow", *Journal of Fluid Mechanics*, Vol. 56, pp. 533-557.

Lamballais, E., Metais, O. and Lesieur, M., 1998, "Spectral-Dynamic Model for Large-Eddy Simulations of Turbulent Rotating Flow", *Theoretical and Computational Fluid Dynamics*, Vol. 12, pp. 149-177.

Launder, B. E., Tselepidakis D. P. and Younis B. A, 1987, "A Second-Moment Closure Study of Rotating Channel Flow", *Journal of Fluid Mechanics*, Vol. 183, pp. 63-75.

Schiestel, R., 1987, "Multiple-Time Scale Modeling of Turbulent Flows in one Point Closures", *Physics of Fluids*, Vol. 30, n°3, pp. 722-731.

Schiestel, R., and Dejoan, A., 2005, "Towards a New Partially Integrated Transport Model for Coarse Grid and Unsteady Turbulent Flow Simulations", *Theoretical and Computational Fluid Dynamics*, Vol. 18, pp. 443-468.

Schiestel, R., 2008, "Modeling and Simulation of Turbulent Flows", *ISTE Ltd and J. Wiley.*

Speziale, C. G., 1979, "Invariance of Turbulent Closures Models", *Journal of Fluid Mechanics*, Vol. 22, n°6, pp. 1033-1037.

Speziale, C. G., 1980, "Closures Relations for the Pressure-Strain Correlation of Turbulence", *Physics of Fluids*, Vol. 23, n°3, pp. 459-463.

Speziale, C. G., Sarkar, S., and Gatski, T. B., 1991, "Modelling the Pressure-Strain Correlation of Turbulence: an Invariant Dynamical Systems Approach", *Journal of Fluid Mechanics*, Vol. 227, pp. 245-272.

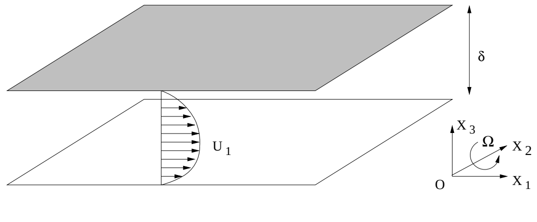

Figure 1: Schematic of fully-developed turbulent channel flow in a rotating frame.

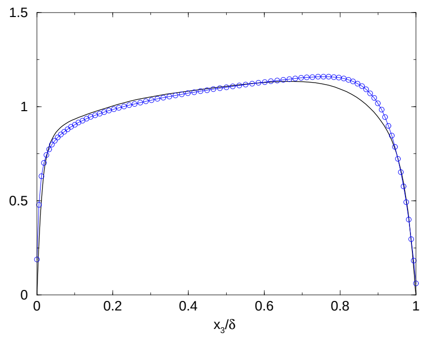

(a)

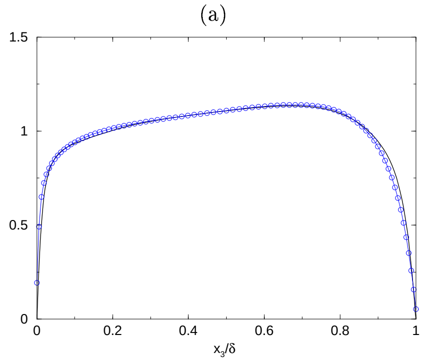

(b)

Figure 2. Mean velocity profile $\langle u_1 \rangle / u_m$ in global coordinate. (a) PITM1 $(24 \times 48 \times 64)$: $\circ$; (b) PITM2 $(84 \times 64 \times 64)$: $\circ$; Highly resolved LES (Lamballais et al., 1998): — . $R_m = 14000$, $Ro_m = 0.17$.

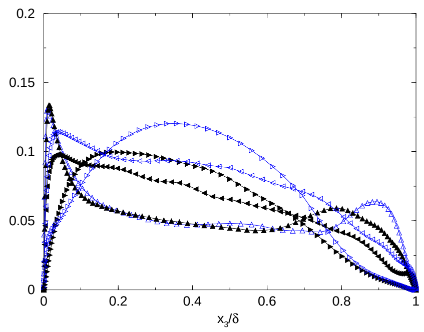

Figure 5: Turbulent Reynolds stresses $\langle \tau_{ii} \rangle^{1/2} / u_m$. PITM2 $(84 \times 64 \times 64)$; $\triangle$: i=1; $\triangleleft$: i=2; $\triangleright$: i=3. Highly resolved LES (Lamballais et al., 1998): $\blacktriangle$:i=1, $\blacktriangleleft$:i=2, $\blacktriangleright$:i=3. $R_m = 14000$, $Ro_m = 0.5$.

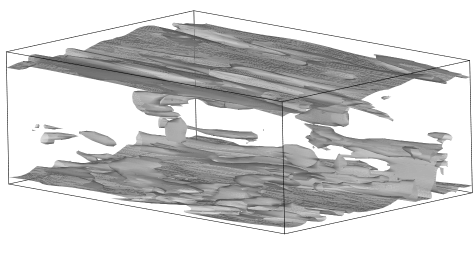

Figure 6: Isosurfaces of vorticity modulus $\omega = 3u_m/\delta$ at $R_m = 14000$ and $Ro_m = 0.17$. PITM1 $(24 \times 48 \times 64)$

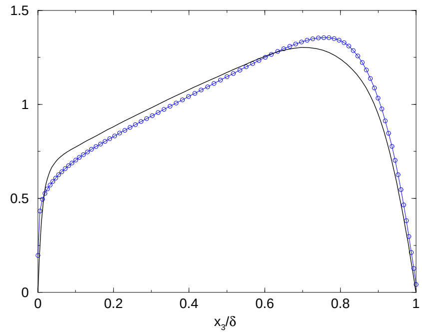

(a)

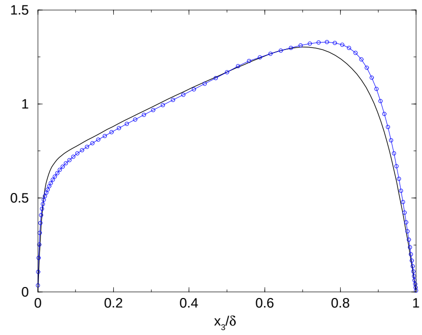

(b)

Figure 3. Mean velocity profile $\langle u_1 \rangle / u_m$ in global coordinate. (a) PITM1 $(24 \times 48 \times 64)$: $\circ$; (b) PITM2 $(84 \times 64 \times 64)$: $\circ$; Highly resolved LES (Lamballais et al., 1998): — . $R_m = 14000$, $Ro_m = 0.5$.

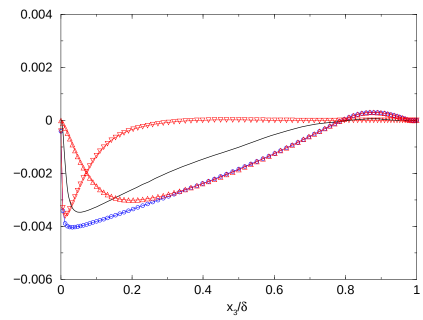

(a)

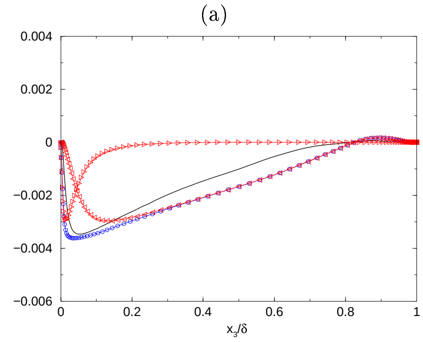

(b)

Figure 4. Turbulent shear stress $\langle \tau_{13} \rangle / u_m^2$. (a) PITM1 $(24 \times 48 \times 64)$; (b) PITM2 $(84 \times 64 \times 64)$; τ_{ij}/u_m^2: $\circ$; $(\tau_{ij})_{sfs}/u_m^2$: $\triangle$; $(\tau_{ij})_{les}/u_m^2$: ∇. Highly resolved LES (Lamballais et al., 1998): — . $R_m = 14000$, $Ro_m = 0.5$.